Light-charged-particle emission in the matched reactions 280 MeV ^{40}Ar+^{27}Al and 670 MeV ^{55}Mn+^{12}C: Coincidence results

Craig M. Brown,[1,*] Zoran Milosevich,[1] Morton Kaplan,[1] Emanuele Vardaci,[1,†] Paul A. DeYoung,[2] James P. Whitfield,[1] Donald Peterson,[2] Christopher Dykstra,[2] Paul J. Karol,[1] and Margaret A. McMahan[3]

[1]*Department of Chemistry, Carnegie Mellon University, Pittsburgh, Pennsylvania 15213*

[2]*Department of Physics, Hope College, Holland, Michigan 49423*

[3]*Lawrence Berkeley National Laboratory, Berkeley, California 94720*

(Received 2 December 1999; published 11 April 2000)

Exclusive measurements of light-charged-particle (^{1}H, ^{2}H, and ^{4}He) energy spectra, angular distributions, and emission multiplicities are reported for the two reactions ^{40}Ar+^{27}Al and ^{55}Mn+^{12}C at a matched excitation energy of 127 MeV. Comparisons are made with statistical model predictions for the evaporative processes in these reactions, which can be characterized as emissions from rotational-energy-dominated systems. The model simulations do well in reproducing a broad range of angular distribution data and the ^{4}He/^{1}H cross-section ratio, using spin distributions derived from fusion cross-section systematics. The same model parameters, however, predict particle energy spectra and coincidence cross sections which are inconsistent with the measurements for both reactions. These results support previous conclusions from model comparisons with inclusive data, and suggest fundamental flaws in the statistical model as applied to light-mass, high-spin, nuclear systems.

PACS number(s): 25.70.Gh, 24.60.Dr, 25.75.Gz

I. INTRODUCTION

In a recent paper [1], we have reported inclusive measurements of light-charged-particle energy spectra and angular distributions for the two matched reactions 280 MeV ^{40}Ar $+^{27}$Al and 670 MeV ^{55}Mn+^{12}C. These reactions produce the same composite nucleus, $^{67}_{31}$Ga*, at an excitation energy ($E_{\mathrm{c.m.}}+Q$) of 127 MeV. From fusion cross-section systematics [2], we expected the composite systems to be formed with angular momenta corresponding to $J_{\max}=54\hbar$ and $42\hbar$ in the two entrance channels, respectively. Comparisons of the inclusive data with predictions from statistical model calculations, however, demonstrated that no unique set of model parameters could give agreement with both the energy spectra and the angular distributions at the same time [1]. The angular distributions were fit reasonably well using $J_{\max}=54\hbar$ and $37\hbar$ for the two reactions, respectively, while the energy spectra required much lower ($25\hbar$) apparent values for this parameter. As discrepancies of this sort had not been seen for heavier nuclear systems ($A\approx150$) [3], it is likely that the relatively small moment of inertia associated with the lighter-mass systems leads to a dominance of rotational effects (rather than Coulomb effects) in the charged-particle emission. In fact, for the reactions studied here, the rotational energy is a substantial fraction of the total excitation energy, a condition which violates assumptions inherent in current model calculations.

In this paper we present the results from particle-particle coincidence (exclusive) measurements for the two reactions 280 MeV ^{40}Ar+^{27}Al and 670 MeV ^{55}Mn+^{12}C, obtained simultaneously with the inclusive data already reported [1]. Although the inclusive studies have been very useful in characterizing emitter properties and in revealing discrepancies with statistical model calculations, the exclusive data provide new dimensionalities for constraints which can rigorously test the models. Such multifaceted comparisons can be particularly important in identifying spin-related properties of the system. In addition, of course, the coincidence requirement strongly favors detection of evaporative particle emissions, and thus serves to filter out contamination, if any, by particles resulting from low-multiplicity noncompound nucleus reactions.

Along with coincidence particle energy spectra and angular distributions, we also report integrated coincidence cross sections for several particle combinations. The corresponding quantities are calculable from statistical model codes, and enable an additional approach to the testing of the models.

The technique of probing the spin of a nuclear system through coincidence measurements has been widely used and well established [4–9]. The method involves one or more ''trigger'' detectors which serve to identify a particle and its emission direction, and a set of ''sweeper'' detectors which measure identified particle spectra at various angles with respect to the trigger particle direction. The location of the trigger and sweeper detectors is critical for studies of angular momentum effects, or spin sensitivity. Typically, two coincidence configurations are employed. The first configuration, called an ''in-plane'' (or IP) coincidence measurement, is intended to determine the particle emission probability at a fixed angle with respect to the spin direction. The second configuration is referred to as an ''out-of-plane'' (or OOP) coincidence measurement, designed to measure the particle emission probability as a function of angle with respect to

*Present address: Lawrence Livermore National Laboratory, P.O. Box 808, L-414, Livermore, CA 94551.

†Present address: Dipartimento di Scienze Fisiche, Università di Napoli Federico II, 80126 Naples, Italy.

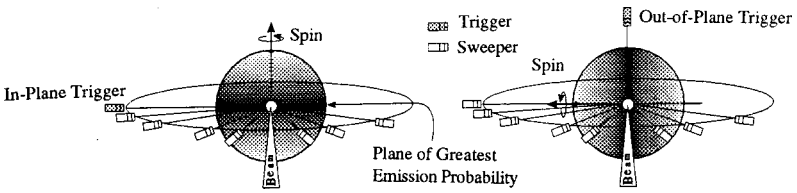

FIG. 1. Schematic representation of spin selection using in-plane and out-of-plane coincidence trigger configurations. In each case the trigger detector is located at 90° to both the spin and beam directions.

the spin direction. These two configurations are illustrated schematically in Fig. 1. In each case the trigger detector is located at 90° to both the spin and beam directions. The particle coincidence rate between a trigger and a sweeper detector is determined by both the nuclear reaction geometry and angular momentum, the latter through the dependence of particle emission probability on the centrifugal barrier. The geometry of the reaction restricts the spin of the compound nucleus (approximately) to a plane perpendicular to the beam, and the centrifugal barrier favors particle emission at 90° to the spin axis. Therefore, in-plane coincidence measurements have the maximum probability of detecting particles emitted at 90° to the spin, as this places both detectors in the plane of greatest emission probability. The out-of-plane coincidence configuration maintains the trigger detector at 90° to the spin, but permits the sweeper detectors to be oriented at various angles from the spin direction. Hence the OOP coincidence rates effectively measure the particle emission probability as a function of angle with respect to the spin. Comparisons of the measured IP and OOP particle coincidence distributions with statistical model simulations then provide a sensitive means for determining the effective spin of the particle-emitting system.

II. EXPERIMENT

The reaction chamber configurations for the exclusive measurements were identical to those described earlier [1] for inclusive studies of the 280 MeV $^{40}Ar+^{27}Al$ and 670 MeV $^{55}Mn+^{12}C$ reactions. Briefly, six or seven solid-state silicon detector telescopes (SSTs) were placed on two concentric turntables at various angles about the beam. These telescopes were used for particle identification and for coincidence measurements between light-charged particles. As the two reactions were carried out in reversed kinematics [10], the particle evaporation spectra could be recorded down to rather low center-of-mass (c.m.) energies by placing the

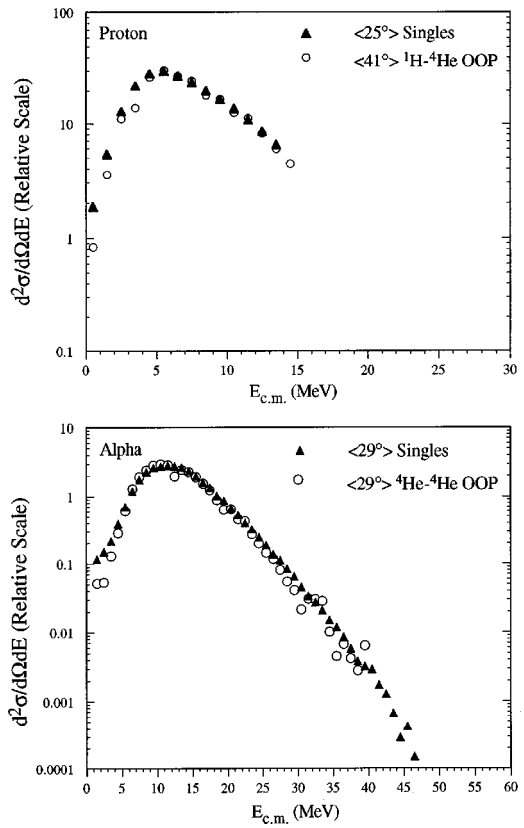

FIG. 2. Comparison of inclusive and exclusive ^{1}H (top) and ^{4}He (bottom) c.m. energy spectra from the 280 MeV $^{40}Ar+^{27}Al$ reaction. The superposed spectra originate from somewhat different spin orientations, yet are indistinguishable in shape.

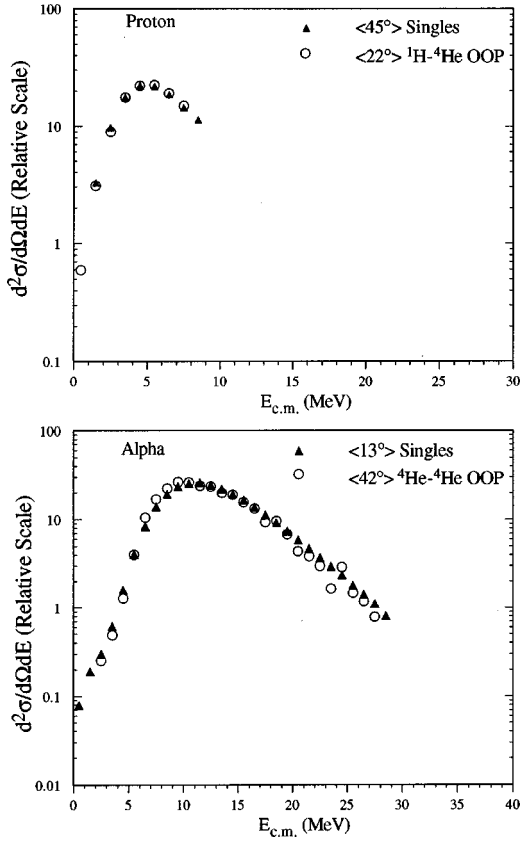

FIG. 3. Comparison of inclusive and exclusive ^{1}H (top) and ^{4}He (bottom) c.m. energy spectra from the 670 MeV $^{55}Mn+^{12}C$ reaction. The superposed spectra originate from somewhat different spin orientations, yet are indistinguishable in shape.

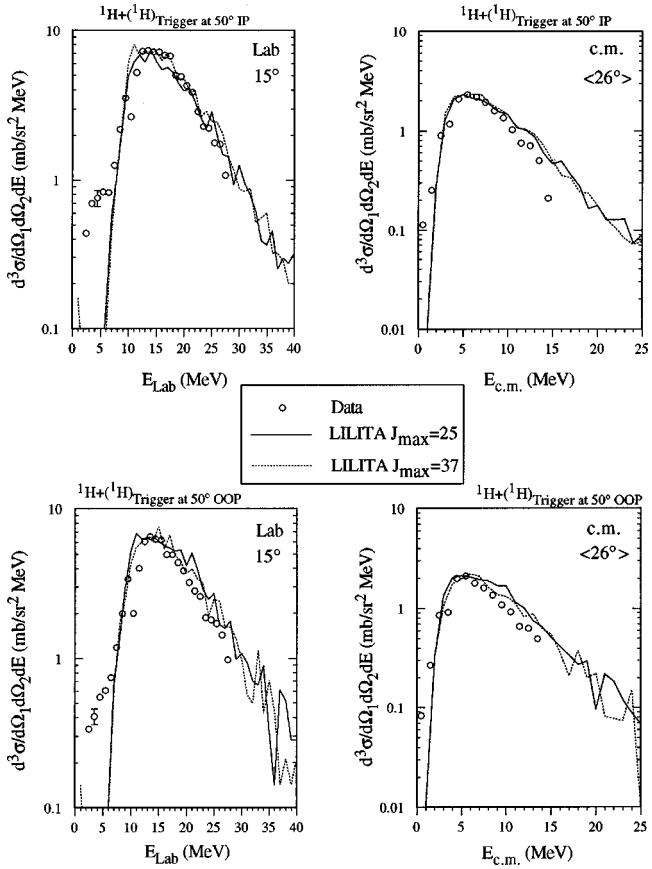

FIG. 4. Proton (^{1}H) energy spectra in coincidence with another ^{1}H recorded in an in-plane (top panels) or an out-of-plane (bottom panels) trigger detector for the 280 MeV ^{40}Ar+^{27}Al reaction. The points are experimental data, and the curves are LILITA_N95 simulations for spin distributions with $J_{\max}$=25 and 37 $\hbar$. The left (right) panels show laboratory (c.m.) energy spectra for both data and calculations.

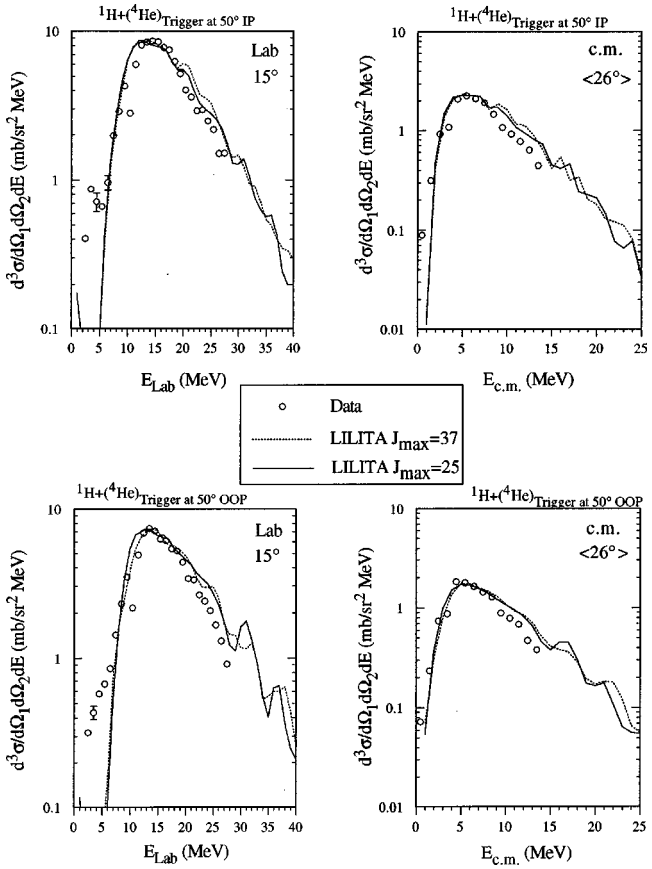

FIG. 5. Proton (^{1}H) energy spectra in coincidence with an α(^{4}He) recorded in an in-plane (top panels) or an out-of-plane (bottom panels) trigger detector for the 280 MeV ^{40}Ar+^{27}Al reaction. Other details as in Fig. 4.

SSTs in the forward hemisphere. In each of the two experiments, an out-of-plane SST and an in-plane SST were configured as trigger detectors at lab angles corresponding to approximately 90° in the c.m. system (50° for the ^{40}Ar +^{27}Al reaction and 35° for the ^{55}Mn+^{12}C reaction). A coincidence event was recorded when two particles were detected simultaneously, one in the trigger detector and the second in one of the sweeper detectors positioned in a plane containing the beam.

The ^{40}Ar and ^{55}Mn beams were produced by the 88-in cyclotron facility at the Lawrence Berkeley National Laboratory, and impinged upon self-supporting targets of Al and C, respectively. For details of chamber geometry, targeting, and detector calibrations, the reader is referred to our earlier paper [1].

III. RESULTS AND DISCUSSION

A. Evidence for statistical emission

As reported in [1], evidence supporting statistical evaporation from equilibrated composite nuclei was found in the shapes of the inclusive c.m. energy spectra for protons and α particles. These spectra were nearly Maxwellian in shape, corresponded to relatively low effective nuclear temperatures, and exhibited constancy of shape over a wide range of c.m. angles. Invariant cross-section maps [11] and c.m. angular distributions [1] of inclusive ^{1}H/^{4}He were also consistent with predominantly evaporative emission.

We show in Figs. 2 and 3, the comparisons of inclusive and exclusive c.m. energy spectral shapes for protons and α's, the exclusive data being generated by simultaneous identification of an α in the trigger detector. Figure 2 gives the comparison for the 280 MeV ^{40}Ar+^{27}Al reaction, and Fig. 3 is for the 670 MeV ^{55}Mn+^{12}C reaction. For both reactions and for both particle types, the shapes of the inclusive and exclusive spectra are nearly identical. Since the coincidence data preferentially select particles originating from equilibrated systems leading to evaporation residues [3,7–9], these comparisons indicate that the exclusive measurements (as well as the inclusive measurements) are relatively free of significant contamination from preequilibrium emissions associated with incomplete fusion reactions. Because of the strongly reversed kinematics in our experiments, such preequilibrium particles are expected to appear at *backward* angles [10,12], well outside the range of our forward angle particle detectors. As incomplete fusion reactions in this energy and mass regime result primarily from preequilibrium

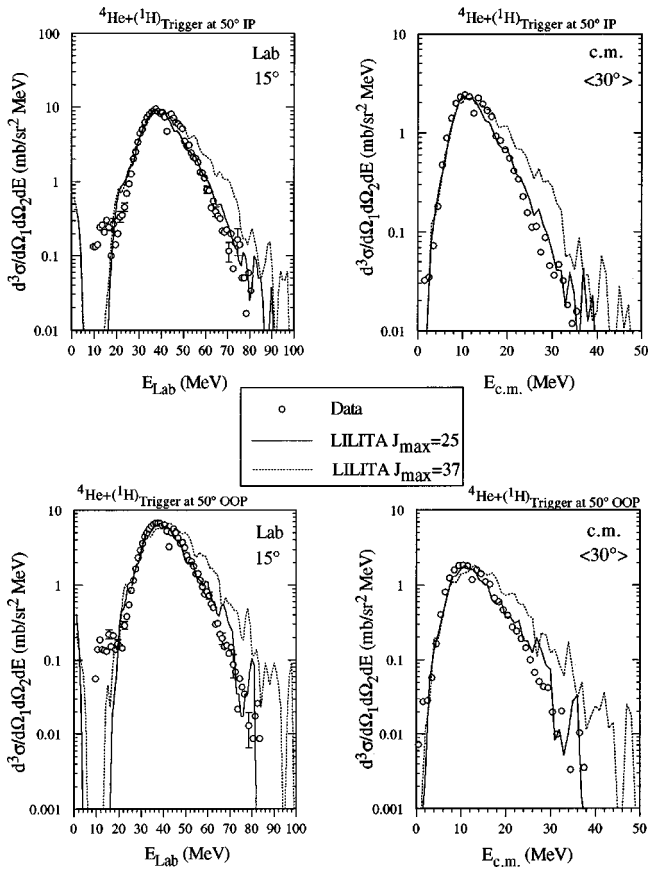

FIG. 6. α(^{4}He) energy spectra in coincidence with a proton (^{1}H) recorded in an in-plane (top panels) or an out-of-plane (bottom panels) trigger detector for the 280 MeV ^{40}Ar+^{27}Al reaction. Other details as in Fig. 4.

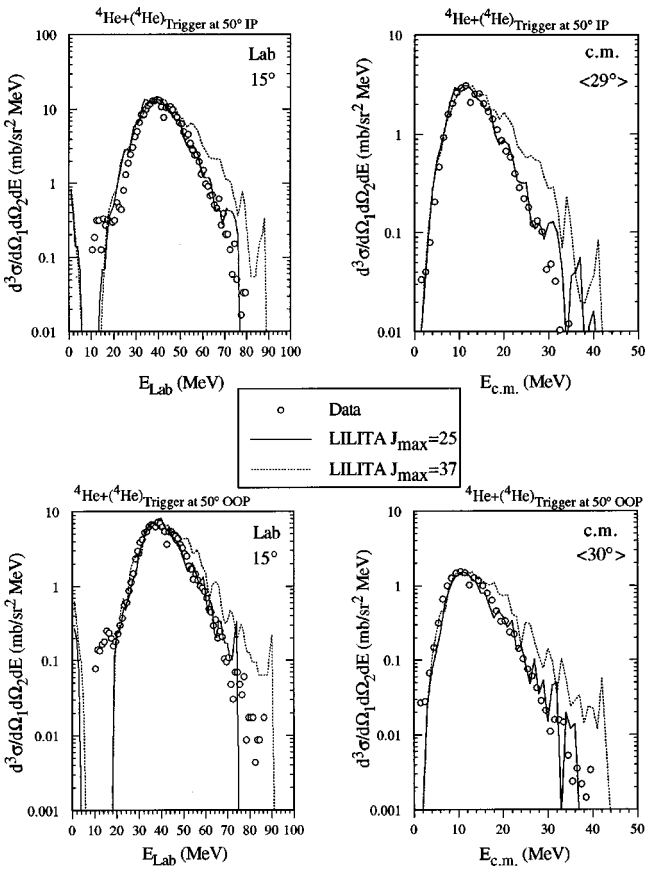

FIG. 7. α(^{4}He) energy spectra in coincidence with another ^{4}He recorded in an in-plane (top panels) or an out-of-plane (bottom panels) trigger detector for the 280 MeV ^{40}Ar+^{27}Al reaction. Other details as in Fig. 4.

particle emission from the target (lighter) nuclei [12,13], we believe that such reactions do not contribute significantly to the observed data. This conclusion is further supported by the nearly identical shapes of the light particle c.m. energy spectra between the two reactions studied here, even though the reaction kinematics (and consequently the transformation Jacobians) are very different. In addition, equilibrium evaporative emissions from incomplete fusion residues would be very strongly *forward* peaked in the laboratory, and no evidence of such distortions is seen in the spectra for either reaction. On the contrary, as shown previously [1], the light particle energy spectra exhibited virtually identical shapes over a wide range of c.m. angles.

B. Comparisons of exclusive measurements to LILITA_N95 simulations

In our earlier paper [1] we presented detailed comparisons of inclusive light-charged-particle data with simulations from two statistical model computer codes, LILITA_N95 [14,15] and MODGAN [16]. These codes contain the same basic physical ingredients and user-selected parameters, but differ in computational methodology and operational characteristics. The versatile LILITA_N95 code [14,15] was used to simulate proton and α evaporative energy spectra, angular distributions, and cross-section ratios. For simulating deuteron and triton evaporation, the MODGAN code [16] was more suitable, and also provided a cross-check with the LILITA_N95 proton and α results. We shall follow a similar procedure here, in comparing the exclusive data with predictions from the statistical model.

A useful feature of the LILITA_N95 code [14,15] is its ability to produce an event-by-event file containing the basic physical quantities which characterize each nuclear reaction event. This file may then be sorted and analyzed (using additional software) according to specific criteria or properties. To simulate coincidence measurements, LILITA_N95 is run in this mode and serves as an event generator. The output event file is then analyzed for particle-particle coincidences, which satisfy the requirements of specified particle types and experimental detector geometry.

The event files generated by LILITA_N95 contain center-of-mass quantities, which are transformed to a specified laboratory frame and checked against the detection criteria (e.g., the positions, acceptance solid angles, and energy thresholds) of the detectors of interest. Hence the simulated reaction is defined by the composition, excitation energy, and angular momentum distribution of the composite (starting) system, and, prior to laboratory transformation, is independent of the target and projectile identities. In the present context, this means that identical event files are produced for both the 280

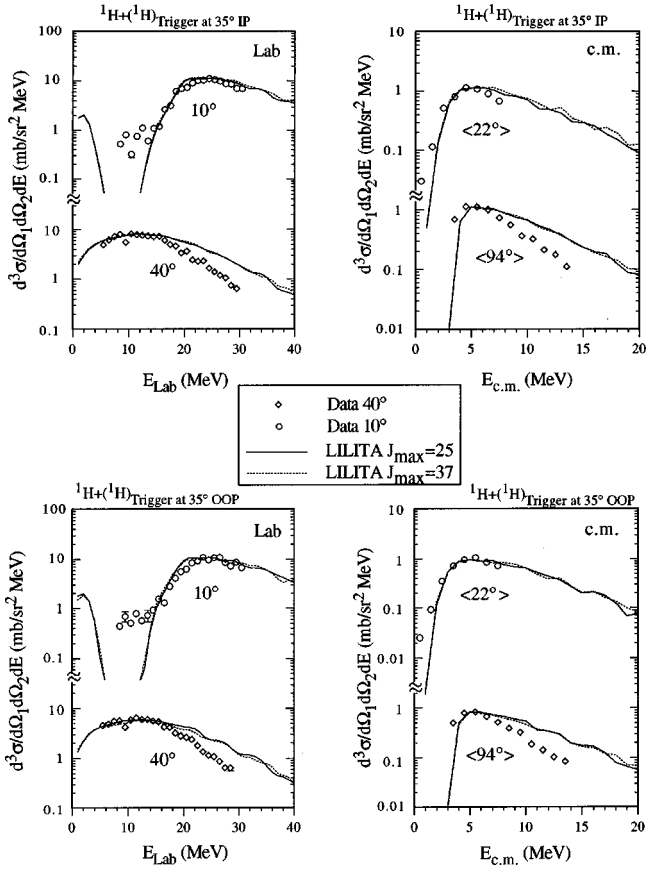

FIG. 8. Proton (^{1}H) energy spectra in coincidence with another ^{1}H recorded in an in-plane (top panels) or an out-of-plane (bottom panels) trigger detector for the 670 MeV ^{55}Mn+^{12}C reaction. The points are experimental data, and the curves are LILITA_N95 simulations for spin distributions with $J_{max}=25$ and 37 $\hbar$. The left (right) panels show laboratory (c.m.) energy spectra for both data and calculations.

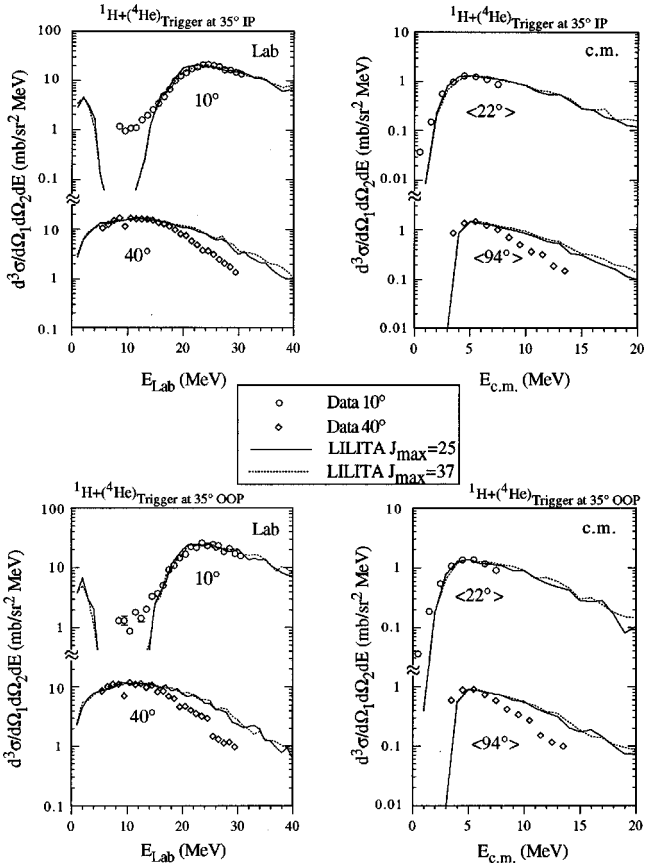

FIG. 9. Proton (^{1}H) energy spectra in coincidence with an α(^{4}He) recorded in an in-plane (top panels) or an out-of-plane (bottom panels) trigger detector for the 670 MeV ^{55}Mn+^{12}C reaction. Other details as in Fig. 8.

MeV ^{40}Ar+^{27}Al and 670 MeV ^{55}Mn+^{12}C reactions, distinguished only by choice of angular momenta. In the comparisons to follow, we shall show experimental and simulated particle energy spectra for each of the two reactions, in both the laboratory and center-of-mass frames, for specific sets of coincidence requirements involving several particle combinations and triggering conditions.

In Figs. 4–7 we present results for the 280 MeV ^{40}Ar+^{27}Al reaction. Figures 4 and 5 display proton (^{1}H) energy spectra in coincidence with a second proton (Fig. 4) or an α(^{4}He) (Fig. 5) detected in a trigger detector. In each figure, the top panels correspond to an in-plane trigger detector and the bottom panels refer to an out-of-plane trigger detector. The points are experimental data, and the curves are LILITA_N95 simulations for spin distributions 0–25 $\hbar$ and 0–37 $\hbar$, as indicated. The left sides of the figures show laboratory energy spectra, and the right sides give the center-of-mass spectra, for both data and calculations. For all four coincidence combinations (particles and trigger positions), the two simulations give about equally satisfactory agreement with the data. This insensitivity of the calculated proton spectra to angular momentum had been noted previously in the analysis of the inclusive data [1]. The slopes of the high-energy portions of the simulations are a little larger (less steep) than the experimental data, a small deviation which could be improved upon by choosing a larger level-density parameter in the model calculations (we used $a=A/10$).

Figures 6 and 7 give comparisons of the α energy spectra for the 280 MeV ^{40}Ar+^{27}Al reaction. The layout is the same as in Figs. 4 and 5, with Fig. 6 showing coincidence data for proton triggers and Fig. 7 giving results for α triggers. Again, laboratory spectra are on the left, c.m. spectra are on the right, in-plane triggers are in the top panels, and out-of-plane triggers are in the bottom panels. The solid curves are spectral simulations with $J_{max}=25\hbar$, and are seen to fit the experimental α spectra very well. The dotted curves are similar calculations but with $J_{max}=37\hbar$, and these are found to be too broad to acceptably reproduce the experimental data. Thus, just like the inclusive comparisons [1], the exclusive LILITA_N95 simulations require a spin parameter $J_{max}=25\hbar$ to reproduce the experimental α energy spectra for all trigger combinations.

Comparisons of LILITA_N95 simulations with the 670 MeV ^{55}Mn+^{12}C coincidence data are shown in Figs. 8–11. The data presentations for this reaction are analogous to those given above in Figs. 4–7, namely proton spectra triggered by protons and α's, respectively, in Figs. 8 and 9, and α spectra

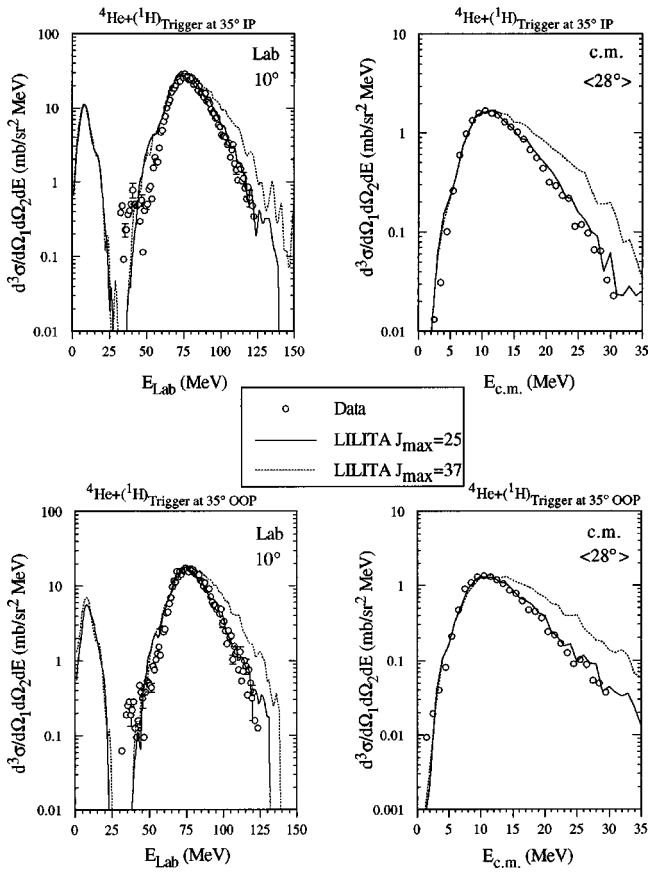

FIG. 10. α(^{4}He) energy spectra in coincidence with a proton (^{1}H) recorded in an in-plane (top panels) or an out-of-plane (bottom panels) trigger detector for the 670 MeV ^{55}Mn+^{12}C reaction. Other details as in Fig. 8.

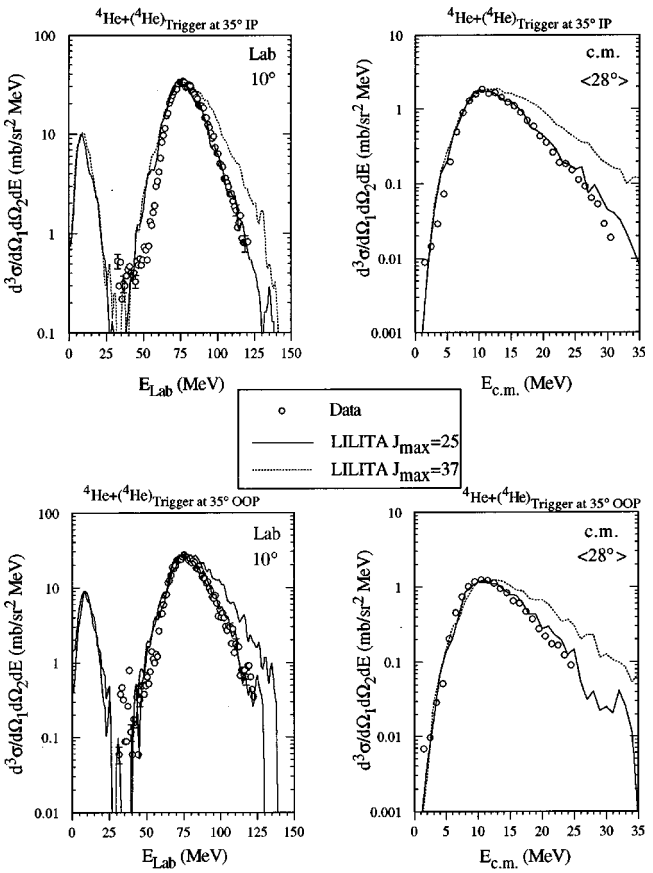

FIG. 11. α(^{4}He) energy spectra in coincidence with another ^{4}He recorded in an in-plane (top panels) or an out-of-plane (bottom panels) trigger detector for the 670 MeV ^{55}Mn+^{12}C reaction. Other details as in Fig. 8.

triggered by protons and α's, respectively, in Figs. 10 and 11. Again, laboratory spectra occupy the left-hand panels and c.m. spectra occupy the right-hand panels, with in-plane triggers in the upper panels and out-of-plane triggers in the lower panels. For each comparison, the simulations were carried out as before with two spin ranges, $J_{max}=25\hbar$ and $37\hbar$. Examination of Figs. 8 and 9 indicates that while the overall agreement between experiment and simulation is not bad, it appears that the simulations underestimate the low-energy part of the proton spectra at the 10° angle and overestimate the high-energy proton data at 40°. The insensitivity of the simulated proton spectra to compound-nucleus spin is seen here as well, precluding the extraction of significant spin information from the proton energy spectral data.

The α energy spectra in Figs. 10 and 11 can be fitted reasonably well by the model simulations with $J_{max}=25\hbar$. Furthermore, the calculated α spectra exhibit the sensitivity to spin distribution seen earlier. It is clear that the LILITA_N95 curve with $J_{max}=37\hbar$ is too broad and deviates considerably from the high-energy sides of the experimental spectra.

In summary, we find that the LILITA_N95 simulations with $J_{max}=25\hbar$ are able to reproduce the exclusive α spectral data in all trigger configurations for both the 280 MeV ^{40}Ar $+^{27}$Al and the 670 MeV ^{55}Mn+^{12}C reactions. The larger spin parameter, $J_{max}=37\hbar$, yields α spectra which disagree with the data in both reactions. Thus it would appear that the spectral comparisons tell us that there is little difference between the spin distributions in the two reactions. However, it is readily demonstrated that this would be an erroneous conclusion. In Fig. 12 we show the experimental c.m angular distributions for ^{4}He in coincidence with another ^{4}He detected in an out-of-plane trigger detector. The open circles are for the 280 MeV ^{40}Ar+^{27}Al reaction and the filled triangles represent data from the 670 MeV ^{55}Mn+^{12}C reaction. It is well known [17–19] that the angular anisotropies of evaporated α's are sensitive to the spins of the emitters, and Fig. 12 reveals almost a factor of 3 difference in the measured anisotropies for the two reactions. These data strongly suggest that the two reactions are associated with significantly different spin distributions in the composite nuclear systems.

In the same way that the exclusive experimental energy spectra are integrated over energy to produce exclusive angular distributions, the simulated coincidence energy spectra derived from sorting LILITA_N95 event-by-event files can be integrated to give the simulated coincidence angular distributions. The coincidence measurement most sensitive to the angular momentum of the emitter is the α-α out-of-plane trigger configuration. Figure 13 shows the ^{4}He-^{4}He exclusive angular distributions (with out-of-plane triggers) for the

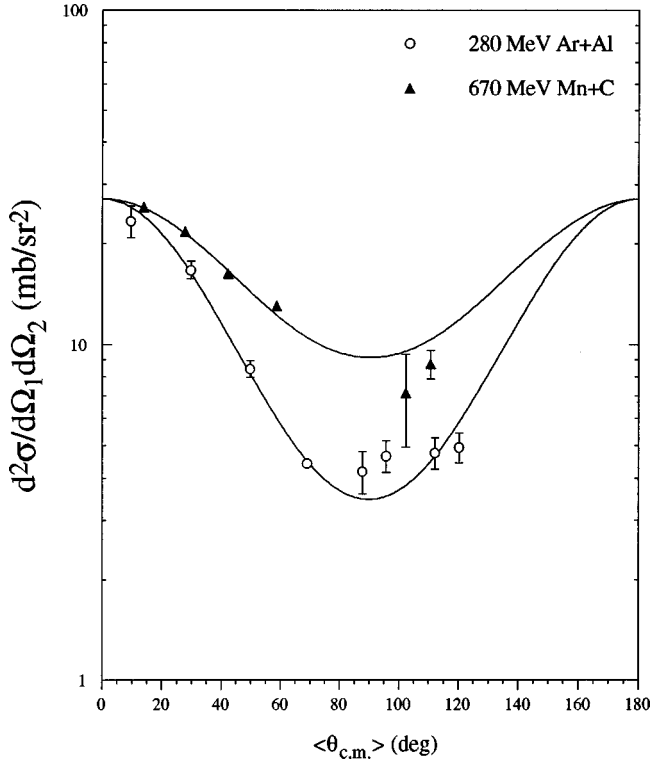

FIG. 12. ^{4}He angular distributions in coincidence with another ^{4}He recorded in an out-of-plane trigger detector for the 280 MeV ^{40}Ar+^{27}Al and 670 MeV ^{55}Mn+^{12}C reactions. In each case the trigger detector was at $\approx 90°$ in the c.m. system. The curves are theoretical fits to guide the eye, and the ^{55}Mn+^{12}C data have been normalized to the ^{40}Ar+^{27}Al data at 0°.

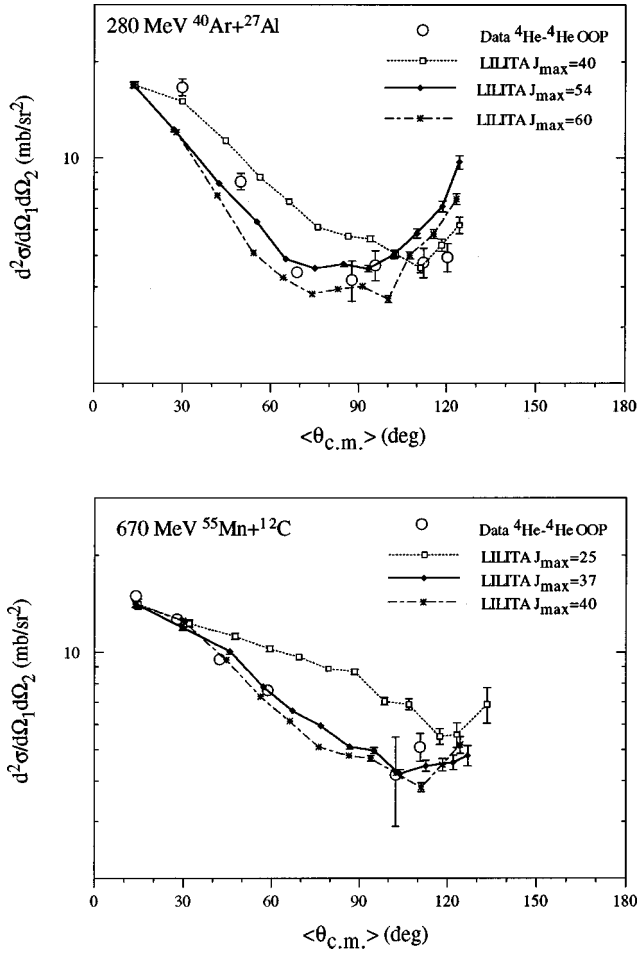

FIG. 13. Exclusive ^{4}He-^{4}He angular distributions for the 280 MeV ^{40}Ar+^{27}Al (top panel) and the 670 MeV ^{55}Mn+^{12}C (bottom panel) reactions, compared to LILITA_N95 simulations. The open circles are the experimental data, and the curves correspond to simulations with spin parameters J_{max} as indicated for each reaction.

two reactions, along with LILITA_N95 simulations for several different spin distributions. The top panel gives the data (as open circles) for the ^{40}Ar+^{27}Al reaction, and the three curves represent simulations with $J_{max}=40$, 54, and 60 $\hbar$, respectively. The bottom panel has corresponding results for the ^{55}Mn+^{12}C reaction, with simulations for $J_{max}=25$, 37, and 40 $\hbar$.

From the comparisons in Fig. 13, the ^{4}He-^{4}He coincidence data for the 280-MeV ^{40}Ar+^{27}Al reaction are fitted fairly well by the simulation for $J_{max}=54\hbar$. The simulated curve for $J_{max}=40\hbar$ is too shallow, while the curve corresponding to $J_{max}=60\hbar$, though deeper, could give reasonable agreement with the data by a small readjustment in the absolute normalization. Thus we conclude that, for this reaction, the simulations yield an effective spin parametrization of $J_{max}=54\pm 6\hbar$.

For the 670 MeV ^{55}Mn+^{12}C reaction, the experimental ^{4}He-^{4}He data (bottom panel in Fig. 13) are very well reproduced by the simulation with $J_{max}=37\hbar$. The spin 40 simulation is a bit more anisotropic than that with spin 37, but also agrees rather well with the experimental angular distribution. The simulation using $J_{max}=25\hbar$ is surely too shallow, compared with the data. Hence from this plot we extract an effective spin parametrization of $J_{max}=37\pm 3\hbar$.

The effective spin parametrizations just derived for the two reactions were based upon comparisons with the ^{4}He-^{4}He out-of-plane exclusive data. It is now of interest to see how well these spin parameters can fit the multiple other combinations of particle coincidences contained in the exclusive data sets. Figure 14 displays the ^{1}H-^{1}H, ^{1}H-^{4}He, ^{4}He-^{1}H, and ^{4}He-^{4}He in-plane and out-of-plane exclusive angular distributions for both the 280 MeV ^{40}Ar+^{27}Al and the ^{55}Mn+^{12}C reactions. The data for ^{40}Ar+^{27}Al are in the left panels and for ^{55}Mn+^{12}C in the right panels. ^{1}H distributions are in the upper panels and ^{4}He distributions are in the lower panels, with each of the specific trigger configurations as indicated. The uncertainties in the data and simulations are given by error bars, and are statistical only. Where error bars are not visible, the statistical uncertainties are smaller than the size of the points. The spin parametrizations used in the simulations were $J_{max}=54\hbar$ for all of the ^{40}Ar+^{27}Al distributions, and $J_{max}=37\hbar$ for the ^{55}Mn+^{12}C distributions.

The exclusive proton angular distributions are all relatively flat for both reactions, with the out-of-plane (OOP) α trigger demonstrating somewhat greater curvature than the other triggers. This is in accord with expectations from the statistical model [17,18,20,21], for spin-driven angular dis-

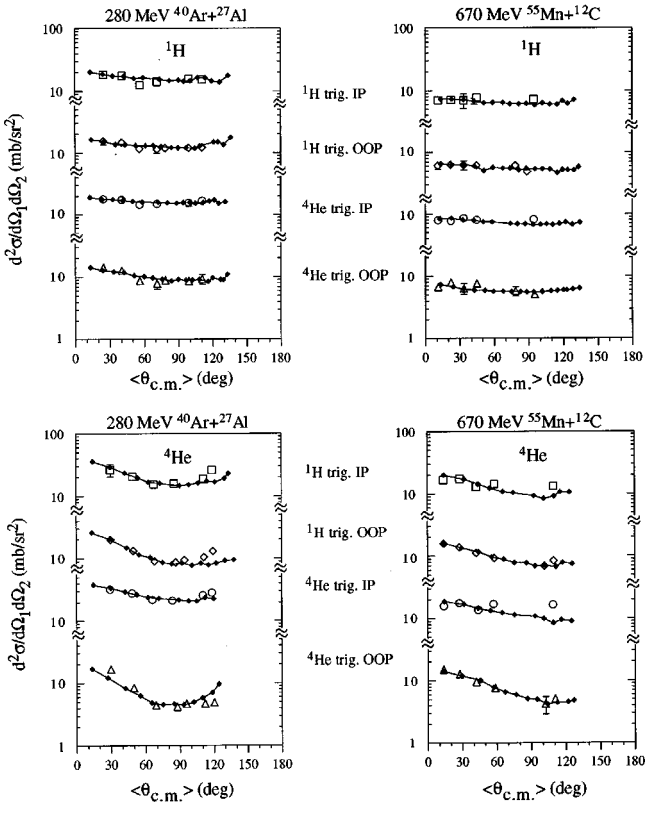

FIG. 14. Exclusive ^{1}H-^{1}H, ^{1}H-^{4}He, ^{4}He-^{1}H, and ^{4}He-^{4}He angular distributions for the 280 MeV ^{40}Ar+^{27}Al (left panels) and the 670 MeV ^{55}Mn+^{12}C (right panels) reactions. The open points are experimental data, and the curves with filled points represent LILITA_N95 simulations with spin parameters $J_{max}=54\hbar$ for Ar+Al and $37\hbar$ for Mn+C.

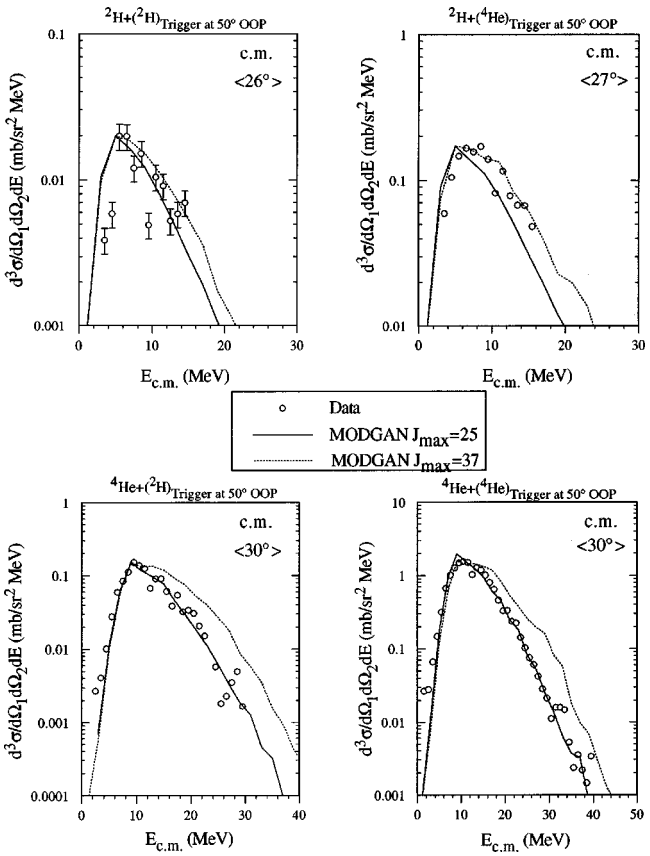

FIG. 15. Energy spectra (c.m.) of deuterons (^{2}H) (top panels) and ^{4}He (bottom panels), in coincidence with trigger ^{2}H (left panels) or trigger ^{4}He (right panels), for the 280 MeV ^{40}Ar+^{27}Al reaction. The curves are MODGAN simulations with spin parameters as indicated.

tributions. In each case the experimental data are well reproduced by the LILITA_N95 simulations, using the stated values of J_{max} for each reaction. The exclusive α angular distributions are also rather well matched by the simulations for both reactions. Small deviations observed at the larger angles probably originate from systematic uncertainties in the integration of incomplete energy spectra, and do not materially alter our conclusions.

To summarize the angular distribution comparisons, we find that a spin parametrization of $J_{max}=54\pm6\hbar$ is required for agreement with the data for the ^{40}Ar+^{27}Al reaction, and a significantly lower value of $J_{max}=37\pm3\hbar$ is needed to match the data for the ^{55}Mn+^{12}C reaction. These results are in sharp contrast with our observations, above, for the α energy spectra, where simulations using these larger spin values yield gross discrepancies with the spectral data. Rather, we showed (Figs. 6, 7, 10, and 11) that the exclusive α spectra for both reactions were reproduced by simulations using $J_{max}=25\hbar$. The inability of the statistical model calculations to fit the particle energy spectra and angular distributions simultaneously, with a single set of parameters, is a glaring deficiency. As reported earlier from inclusive measurements [1], the difficulty appears in applying the model to relatively light-mass, high-spin systems, where the rotational energy is not small compared to the thermal energy.

C. Comparisons of exclusive measurements to MODGAN simulations

The MODGAN statistical model code [16] generates evaporative particle decay chains using the same basic physical ingredients as LILITA_N95, but with considerably different methodology. The code calculates particle coincidence energy spectra and angular distributions by sampling the decay chains in conjunction with geometrical definitions of laboratory trigger and sweeper detectors. In this section, we shall present data and MODGAN simulations involving deuterons (^{2}H) and α particles (^{4}He). Comparisons will be made for out-of-plane (OOP) triggered coincidences between ^{2}H-^{2}H, ^{2}H-^{4}He, ^{4}He-^{2}H, and ^{4}He-^{4}He. The deuteron coincidences extend the simulation comparisons beyond what can be readily achieved with the LILITA_N95 code, and the α-α coincidence simulations serve to compare the MODGAN results with those from LILITA_N95.

Figure 15 gives c.m. energy spectra of deuterons (top panels) and α's (bottom panels) in coincidence with OOP trigger ^{2}H (left panels) or OOP trigger ^{4}He (right panels) for the 280 MeV ^{40}Ar+^{27}Al reaction. The open circles are experimental data and the solid and dashed curves are MODGAN simulations with $J_{max}=25$ and 37 $\hbar$, respectively. The ^{2}H data (top panels) show considerable scatter, making it diffi-

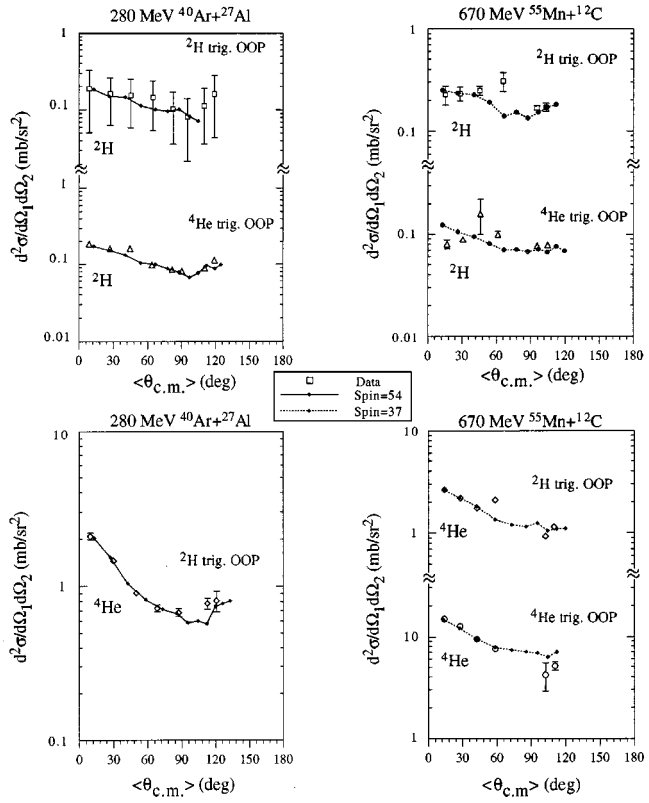

FIG. 16. Exclusive ^{2}H-^{2}H, ^{2}H-^{4}He, and ^{4}He-^{4}He c.m. angular distributions for the 280 MeV ^{40}Ar+^{27}Al (left panels) and the 670 MeV ^{55}Mn+^{12}C (right panels) reactions. The open points are experimental data and the curves are MODGAN simulations with $J_{\max}=54\hbar$ for Ar+Al and $37\hbar$ for Mn+C.

cult to uniquely distinguish between the two calculated curves. However, the ^{4}He data triggered by OOP deuterons (bottom left) clearly show the $J_{\max}=25\hbar$ curve to be the better fit. The same can be unambiguously stated for the ^{4}He-^{4}He results (bottom right), in full agreement with the LILITA_N95 comparison made in Fig. 7 above.

Exclusive ^{2}H-^{2}H, ^{2}H-^{4}He, and ^{4}He-^{4}He c.m. angular distributions are shown in Fig. 16. The left-hand panels are for the 280 MeV ^{40}Ar+^{27}Al reaction and the right-hand panels are for the 670 MeV ^{55}Mn+^{12}C reaction. The open points are experimental data and the curves connecting filled points are the MODGAN simulations with $J_{\max}=54\hbar$ for ^{40}Ar+^{27}Al and $J_{\max}=37\hbar$ for ^{55}Mn+^{12}C. The excellent agreement between these angular distribution data and the MODGAN simulations strongly supports the conclusions reached above from comparisons with the LILITA_N95 simulations.

D. Comparisons of particle-particle cross-section ratios

We have described, above, comparisons between measurements and statistical model predictions for particle-particle coincidence energy spectra and angular distributions. These comparisons essentially test the ability of the model to reproduce the observed spectral shapes. An additional, and very useful, comparison may also be made by integrating the angular distributions to yield coincidence cross sections for the various particle combinations. While the experimental data are able to provide absolute coincidence cross sections, the model calculations have no built-in absolute normalization and therefore give coincidence multiplicities rather than cross sections. To avoid introducing an unnecessary uncertainty, we shall compare our data with model simulations in terms of cross-section ratios, in each case using the appropriate integrated proton inclusive cross section as the normalizing factor.

The cross-section ratios predicted by the LILITA_N95 code are given in Table I for different values of the spin-distribution parameter $J_{\max}$, listed in the first column. The second column presents the calculated *inclusive* α-to-proton ratios, and columns 3, 4, and 5 show, respectively, the α-α, proton-α, and proton-proton coincidence cross sections, relative to the calculated inclusive proton cross sections. The trends with spin predicted by the simulations are qualitatively what one would expect from the statistical model. With increasing spin, α emission becomes increasingly favored over proton emission, and hence the ratios (^{4}He/^{1}H), (^{4}He-^{4}He)/^{1}H, and (^{1}H-^{4}He)/^{1}H all increase. The last column in Table I, (^{1}H-^{1}H)/^{1}H, shows the opposite behavior, decreasing systematically as $J_{\max}$ increases.

TABLE I. Comparison of experimental cross-section ratios with statistical model predictions.

$J_{\max}$ ($\hbar$)	(^{4}He/^{1}H)	(^{4}He-^{4}He)/^{1}H	(^{1}H-^{4}He)/^{1}H	(^{1}H-^{1}H)/^{1}H
		LILITA_N95		
15	0.35	0.30	0.89	2.31
25	0.45	0.46	1.10	2.21
37	0.66	0.87	1.38	1.92
40	0.74	1.03	1.46	1.84
54	1.21	2.10	1.76	1.40
60	1.41	2.68	1.91	1.34
		Experimental data		
^{40}Ar+^{27}Al	1.16±0.12	0.35±0.10	0.99±0.21	0.45±0.10
^{55}Mn+^{12}C	0.79±0.12	0.27±0.04	0.71±0.11	0.18±0.04

Below the model simulation ratios in Table I we present the *experimental* cross-section ratios measured for the 280 MeV ^{40}Ar+^{27}Al and the 670 MeV ^{55}Mn+^{12}C reactions. For the (^{4}He/^{1}H) inclusive ratios, the ^{40}Ar+^{27}Al data are consistent with the model calculation for $J_{max}=54\hbar$, and the ^{55}Mn+^{12}C data are close to the calculated value for $J_{max}=40\hbar$. Hence, the experimental (^{4}He/^{1}H) ratios for both reactions require spin distributions (from the model calculations) which are in good agreement with the results from the angular distribution comparisons discussed above. The estimated uncertainties in the measured ratios are small enough to preclude overlap with the J_{max} values needed to fit the particle energy spectra. However, there is no agreement between any of the measured coincidence cross-section ratios and the simulations, which appear to suggest a rather low J_{max} value from the (^{4}He-^{4}He)/^{1}H and (^{1}H-^{4}He)/^{1}H ratios and an unreasonably high J_{max} value from the (^{1}H-^{1}H)/^{1}H ratio. Thus there is a clear failure of the model calculations to reproduce the experimental particle-particle coincidence cross sections.

IV. CONCLUSIONS

In this work we have compared the measured light-charged-particle coincidence energy spectra and angular distributions with simulations based upon the statistical model, for the matched reactions 280 MeV ^{40}Ar+^{27}Al and 670 MeV ^{55}Mn+^{12}C. The focus here is on relatively light mass systems, for which the angular momentum is expected to play a dominant role in the evaporation processes. For simulations involving at least one detected α particle, the calculations show significant sensitivity to the entrance channel spin. The computed results are in good agreement with the angular distribution data for both reactions, when appropriate values of the spin parameter J_{max} are chosen from fusion cross-section systematics for each reaction. In contrast, the particle energy spectra require much lower apparent spins, and do not appear to differentiate between entrance channel spins in the two reactions. This major discrepancy is consistently observed between the spectral data and the angular distribution data, involving multiple coincidence triggers and several combinations of particles. While the comparisons reported here are derived from particle-particle exclusive data, which effectively eliminate contamination from nonevaporative processes, the results obtained support and confirm the conclusions reported previously from particle-inclusive data [1].

The light-particle emission multiplicities, as reflected in the particle cross-section ratios, have provided another degree of freedom for testing the predictions of the statistical model. The measured inclusive α/proton cross-section ratios for the 280 MeV ^{40}Ar+^{27}Al and the 670 MeV ^{55}Mn+^{12}C reactions can be reproduced by the model simulations using the spin distributions derived from the corresponding angular distribution data. The coincidence cross sections, however, involving two α's, two protons, or one α and one proton, cannot be reproduced by the simulations with any consistent set of spin parameters. Hence the cross-section comparisons have brought to light, from another vantage point, the result that serious deficiencies exist in the statistical model as commonly conceived [21].

ACKNOWLEDGMENTS

This paper is based upon the Ph.D. thesis of Craig M. Brown, Carnegie Mellon University, 1997 (unpublished). We would like to thank the staff of the LBNL 88-Inch Cyclotron for excellent support in carrying out these experiments, and Bill Rathbun for invaluable assistance with the data acquisition system and electronics. N.N. Ajitanand was very helpful in the operation and debugging of the MODGAN code. This work was supported by the Division of Nuclear Physics, U.S. Department of Energy, and the National Science Foundation.

[1] C.M. Brown, Z. Milosevich, M. Kaplan, E. Vardaci, P. DeYoung, J.P. Whitfield, D. Peterson, C. Dykstra, P.J. Karol, and M.A. McMahan, Phys. Rev. C **60**, 064612 (1999).

[2] P. Frobrich, Phys. Rep. **116**, 337 (1984).

[3] W.E. Parker, M. Kaplan, D.J. Moses, G. La Rana, D. Logan, R. Lacey, J.M. Alexander, D.M. de Castro Rizzo, P. DeYoung, R.J. Welberry, and J.T. Boger, Phys. Rev. C **44**, 774 (1991), and references cited therein.

[4] J. Boger, J.M. Alexander, R.A. Lacey, and A. Narayanan, Phys. Rev. C **49**, 1587 (1994).

[5] M. Kaplan, C. M. Brown, J. B. Downer, Z. Milosevich, E. Vardaci, J. P. Whitfield, C. Copi, and P. DeYoung, *Advances in Nuclear Dynamics*, edited by W. Bauer and A. Mignerey (Plenum, New York, 1996), p. 113.

[6] W. Kuhn, R. Albrecht, H. Damjantschitsch, H. Ho, I. Rode, R.M. Ronningen, F. Scheibling, J. Slemmer, and J.P. Wurm, Z. Phys. A **298**, 95 (1980).

[7] R. Lacey, N.N. Ajitanand, J.M. Alexander, D.M. de Castro Rizzo, P. DeYoung, M. Kaplan, M. Kildir, L. Kowalski, G. La Rana, D.J. Moses, D. Logan, W.E. Parker, G.F. Peaslee, L.C. Vaz, and M.S. Zisman, Phys. Rev. C **37**, 2561 (1988).

[8] W.E. Parker, M. Kaplan, D.J. Moses, J.M. Alexander, R.A. Lacey, D.M. de Castro Rizzo, J. Boger, A. Narayanan, G.F. Peaslee, and D.G. Popescu, Nucl. Phys. **A594**, 1 (1995).

[9] G.F. Peaslee, N.N. Ajitanand, J.M. Alexander, M. Kaplan, M. Kildir, R. Lacey, D. Logan, D.J. Moses, L.C. Vaz, and M.S. Zisman, Phys. Rev. C **39**, 488 (1989).

[10] D.J. Moses, M. Kaplan, J.M. Alexander, D. Logan, M. Kildir, L.C. Vaz, N.N. Ajitanand, E. Duek, and M.S. Zisman, Z. Phys. A **320**, 229 (1985).

[11] C.M. Brown, Ph.D. thesis, Carnegie Mellon University, 1997 (unpublished).

[12] M.F. Vineyard, S.E. Atencio, J.F. Crum, G.P. Gilfoyle, B.G. Glagola, D.G. Henderson, D.G. Kovar, C.F. Maguire, J.F. Mateja, R.G. Ohl, F.W. Prosser, J.H. Rollinson, and R.S. Trot-

ter, Phys. Rev. C **49**, 948 (1994).
[13] M. Dasgupta, D.J. Hinde, N. Rowley, and A.M. Stefanini, Annu. Rev. Nucl. Part. Sci. **48**, 401 (1998).
[14] The code LILITA_N95 is an extensively modified version of the LILITA program originally developed by J. Gomez del Campo [15]. It has been renamed to differentiate it from several other versions of LILITA [M. Kaplan and G. La Rana (private communication)].
[15] J. Gomez del Campo and R.G. Stokstad, Oak Ridge National Laboratory Report ORNL-TM-7295 1981; J. Gomez del Campo, R.G. Stokstad, J.A. Biggerstaff, R.A. Dayras, A.H. Snell, and P.H. Stelson, Phys. Rev. C **19**, 2170 (1979).
[16] N.N. Ajitanand and J.M. Alexander, Nucl. Instrum. Methods Phys. Res. A **376**, 213 (1996).
[17] T. Ericson, Adv. Phys. **9**, 425 (1960).
[18] T. Dossing, Licentiat thesis and unpublished notes, University of Copenhagen, Denmark (1977).
[19] G. Catchen, M. Kaplan, J.M. Alexander, and M.F. Rivet, Phys. Rev. C **21**, 940 (1980).
[20] D. Bodansky, Annu. Rev. Nucl. Sci. **12**, 79 (1962).
[21] R.G. Stokstad, in *Treatise on Heavy Ion Science*, edited by D.A. Bromley (Plenum, New York, 1985), Vol. 3, p. 83.